JACS
JOURNAL OF THE AMERICAN CHEMICAL SOCIETY
Article
pubs.acs.org/JACS

Fractal Surfaces of Molecular Crystals Mimicking Lotus Leaf with Phototunable Double Roughness Structures

Ryo Nishimura,[†] Kengo Hyodo,[†] Haruna Sawaguchi,[‡] Yoshiaki Yamamoto,[‡] Yoshimune Nonomura,[‡] Hiroyuki Mayama,[*,∥] Satoshi Yokojima,[§,⊥] Shinichiro Nakamura,[⊥] and Kingo Uchida[*,†]

[†]Department of Materials Chemistry, Ryukoku University, Seta, Otsu, Shiga 520-2194, Japan

[‡]Department of Biochemical Engineering, Graduate School of Science and Engineering, Yamagata University, 4-3-16, Jo-nan, Yonezawa, Yamagata 992-8510, Japan

[∥]Department of Chemistry, Asahikawa Medical University, 2-1-1-1, Midorigaoka-higashi, Asahikawa, Hokkaido 078-8510, Japan

[§]School of Pharmacy, Tokyo University of Pharmacy and Life Sciences, 1432-1 Horinouchi, Hachioji, Tokyo 192-0392, Japan

[⊥]RIKEN Innovation Center, Nakamura Laboratory, 2-1 Hirosawa, Wako, Saitama 351-0198, Japan

Supporting Information

ABSTRACT: Double roughness structure, the origin of the lotus effect of natural lotus leaf, was successfully reproduced on a diarylethene microcrystalline surface. Static superwater-repellency and dynamic water-drop-bouncing were observed on the surface, in the manner of natural lotus leaves. Double roughness structure was essential for water-drop-bouncing. This ability was not observed on a single roughness microcrystalline surface showing the lotus effect of the same diarylethene derivative. The double roughness structure was reversibly controlled by alternating irradiation with UV and visible light.

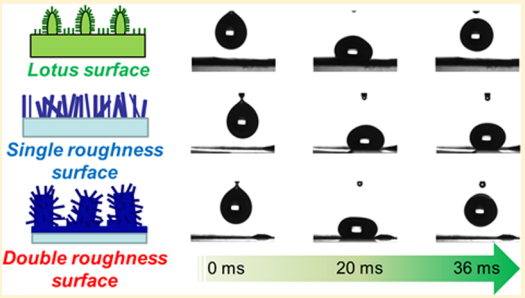

INTRODUCTION

In nature, many plants and insects have superhydrophobic surfaces (water contact angles (CAs) larger than 150°) with double roughness structure. For example, the lotus leaf and legs of a water strider have the double roughness structure. Here, the double roughness structure is the origin of the superhydrophobic lotus effect which is useful for self-cleaning materials and floating ability on a water surface. We started this research to clarify the importance of the structure.[1,2] Historically, the most important finding is the "lotus effect" by Barthlott and Neinhuis.[2] They investigated the superwater-repellent and self-cleaning effect of the lotus leaf and attributed it to the double roughness surface structure with micro- and nanostructures (trichomes, cuticular folds, and wax crystals), together with the hydrophobic properties of epicuticular wax.[3] Since air pockets are maintained in the structure, a water droplet can move more easily, and the structure induces the self-cleaning effect.

On the other hand, the bouncing of a water drop on the lotus leaf also plays an important role in self-cleaning, and artificial double roughness structures have been prepared.[4] Parkin et al. fabricated superhydrophobic self-cleaning surfaces with the dual-scale nature of TiO_2 nanoparticles, and demonstrated that self-cleaning is based on surface micro/nanomorphologies.[4a] Here, we report a guiding principle to prepare the double roughness structure of a diarylethene microcrystalline surface with superhydrophobicity and the ability to bounce a water droplet on it.

Recently, much attention was paid to the stimuli-responsive organic crystals. Naumov et al. discovered photo- and thermosalient organic crystals, and many types of mechanically responsive molecular crystals were reviewed.[5] Burgess et al. reported the phototunable wetting of hybrid materials with inverse opal structures.[6] In previous papers, we controlled surface topography on the microcrystalline surface of a thermally irreversible photochromic diarylethene **1o** (Figure 1),[7−9] which has the photoreactivity in the crystalline state.[10] Upon UV irradiation to the microcrystalline **1o** film, needle-shaped crystals of **1c** grew on the surface, and a superhydrophobic lotus effect was observed. Then these crystals were melted upon irradiation with visible light, and the lotus effect disappeared.

Surface wettability depends on crystal sizes. While controlling the needle-shaped crystals of **1c** to around 1−2 μm in diameter and 10 μm in length by keeping the surface at 30 °C for 24 h in the dark, a superwater-repellant lotus effect was observed (contact angle (CA) and the sliding angle (SA) of a water droplet was about 163° and 2°, respectively). In contrast, a surface covered with needle-shaped crystals and rod-shaped crystals (diameters and lengths approximately 5−10 μm and 20−30 μm, respectively) was prepared by two steps of UV irradiation and thermal control. The surface showed the property to adhere a water droplet, i.e., the rose-petal effect

Received: June 6, 2016
Published: July 25, 2016

DOI: 10.1021/jacs.6b05562
J. Am. Chem. Soc. 2016, 138, 10299−10303

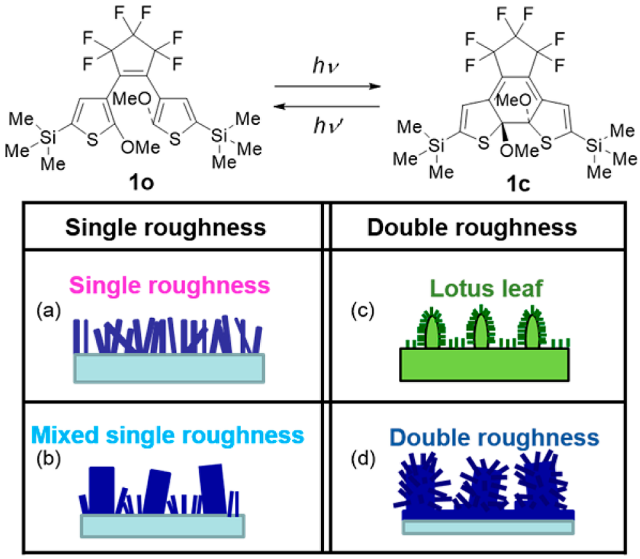

Figure 1. Molecular structures of the open- and closed-ring isomers of a photochromic diarylethene **1**, and four different surface structures. A single roughness surface of the diarylethene (a), a mixed single roughness surface of the diarylethene (b), the double roughness surface of natural lotus leaf (c), a double roughness surface of the diarylethene (d).

(CA = 154° but with a water droplet pinned on the surface, Figure S3).[8,9] The topography of those superhydrophobic surfaces was single roughness structures.[11−13]

RESULTS AND DISCUSSION

Here, we prepared a photoresponsive superhydrophobic surface with double roughness structures using the same diarylethene **1o** shown in Figure 1. Initially the microcrystalline surface of **1o** (Figure 2-1) was irradiated with UV light. Due to photoisomerization, the colorless **1o** near the surface became blue **1c** (Figure 2-2). Then, the needle-shaped crystals of **1c** grew on the surface by storage at 50 °C (Figure 2-3). After storage for 24 h at 50 °C in the dark, the surface was covered with rod-shaped crystals of **1c** (Figure 2-4). The topographical change on the surface is due to Ostwald ripening.[8] To make the double roughness structure, we assumed that thicker rod-shaped crystals would not melt upon visible light irradiation and could play the role of a larger-sized structure of the double roughness structure.

In order to make fat (thick) rod-shaped crystals of **1c**, we further applied this Ostwald ripening. We again irradiated the surface in Figure 2-4 with UV light and stored it at 70 °C for 3 h in the dark (Figure 2-5): the small rod-shaped crystals of **1c** grew from the newly generated **1c** on the surface (Figure 2-6), and they were incorporated in the larger rod-shaped crystals (Figure 2-7a). The rod-shaped crystals, especially small ones, grew in size (Figure S5). The average width and length of these rod-shaped crystals at the state shown in Figure 2-7a were 10 and 21 μm, respectively (Figure S6).

Upon visible light irradiation to the surface of the Figure 2-7a state, cycloreversion reaction from **1c** to **1o** proceeded, and the surface was covered with cubic-shaped crystals of **1o** (Figure 2-8a) on the 10-μm rough structures. The size of each bumpy rod-shaped crystal was almost the same as that of a projection on a lotus leaf covered with plant wax tubes. As expected, the enlarged crystals were not melted: otherwise, the smaller rod-shaped crystals of **1c** would be lost due to Ostwald ripening or

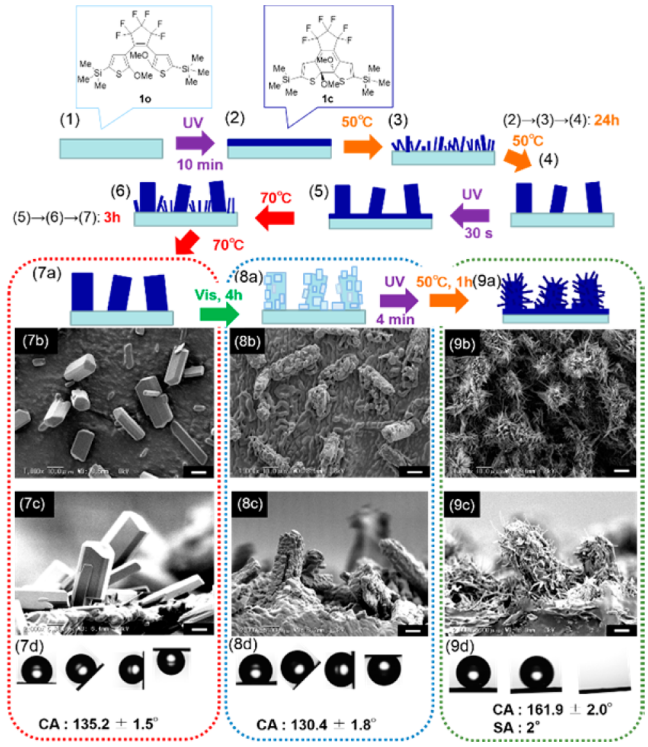

Figure 2. Preparation of lotus surface with double roughness structures (1−9a): pale blue and dark blue parts correspond to crystals of **1o** and **1c**, respectively. SEM images of each surface: (7b) surface with rod-shaped crystals of **1c**, (8b) after visible light irradiation to surface of 7b, (9b) after second UV irradiation to the surface of 7b followed by storing at 50 °C for 1 h in dark; (7c, 8c, 9c) the side view of the surfaces of 7b, 8b, 9b, respectively; (7d, 8d, 9d) water droplet (1.5 μL) on surfaces of 7b, 8b, and 9b, respectively. Scale bars, 10 μm for 7b−9b images, which are magnified 1000 times; 5 μm for 7c−9c images, which are magnified 2000 times.

melted to form a flat surface upon visible light irradiation.[8,9] Upon UV irradiation to the surface, each rod-shaped crystal was covered with needle-shaped crystals of **1c** of 0.2−0.5 μm width and 3−5 μm length, and double roughness structures were prepared (Figure 2-9a). The needle-shaped crystals were much smaller than those grown on the flat microcrystalline surface of **1o**. This is due to the small supply of **1c** crystals to form needle-shaped crystals on each projection. Figure 2-7b,8b,9b shows SEM images of the surfaces of the states shown in Figure 2-7a,8a,9a, and Figure 2-7c,8c,9c shows SEM images of cross sections of samples in Figure 2-7b,8b,9b. The distribution of the sizes of the microstructures on natural lotus leaf was reported by using box-counting fractal analysis.[14] The size distribution of the double roughness structure was very similar to that of natural lotus leaf (Figure S7).

The CAs of water droplets on the surfaces of rod-shaped crystals of **1c** (Figure 2-7a,7b,7c) and cubic crystals of **1o** (Figure 2-8a,8b,8c) were around 130°, and water droplets were pinned on the surface, even when the surfaces were upside down (Figure 2-7d,8d). After formation of double roughness structures, CA and SA on the surface changed to 161.9 ± 2.0° and 2°, respectively. The advanced (CA_{ad}) and receding (CA_{rec}) CAs of a water droplet were 162.0 ± 1.6° and 158.3 ± 1.4°, respectively. Thus, a remarkable lotus effect was observed (Figure 2-9d). The reversibility of the melting and reformation of double roughness structure by alternate

DOI: 10.1021/jacs.6b05562
J. Am. Chem. Soc. 2016, 138, 10299−10303

irradiation of visible and UV light were successfully achieved as well (Figure S9).

With a change to the sequence of the irradiation of visible and UV light (Figure 3), no surface with double roughness

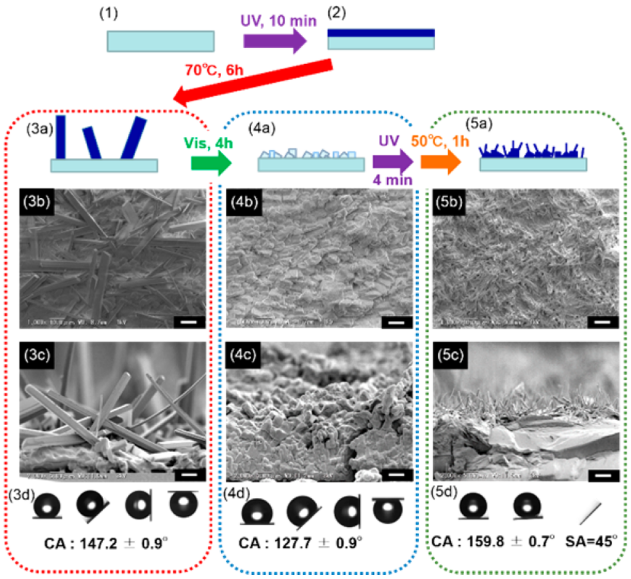

Figure 3. Procedure for making rod-shaped crystals (1−5a). By UV irradiation of initial surface of **1o** (1) followed by heating the state of (2) at 70 °C, a rough surface covered with rod-shaped **1c** was formed (3a). A surface covered with cubic crystals of **1o** was generated upon visible light irradiation to 3a for 4 h (4a). The surface (5a) was prepared by 4 min of UV irradiation and crystal growth of **1c** by storage at 40 °C for 1 h in the dark. SEM images corresponding to 3a, 4a, and 5a are shown in 3b, 4b, and 5b, respectively. Also, the cross-section images of 3b, 4b, and 5b are shown in 3c, 4c, and 5c, respectively. Water droplets (1.5 μL) on surfaces 3b, 4b, and 5b are shown in 3d, 4d, and 5d, respectively. Scale bars, 10 μm for 3b−5b images, which are magnified 1000 times; 5 μm for 3c−5c images, which are magnified 2000 times.

structure was prepared. This indicates that it is important to prepare thick rod-shaped crystals to form a double roughness structure. The surface with thinner rod-shaped crystals (Figure S6) resulted in a surface with a single roughness structure (Figure 3-5a). We found that **1c** remained in the core of the thick rod-shaped crystal (Figure 2-7a) by XRD spectrum (Figure S10). The distinct difference between the surface wettability of Figure 2-9b and Figure 3-5b shows the critical role of the double roughness structures in wettability. This difference is attributable for the larger fractal dimension of double roughness structures in a 0.5−2.4 μm sized area (compare Figures S7b and S8). Also, existence of large air pockets allows intrusion of water to the pockets.

The static CAs and SAs of the microcrystalline surface with double roughness structure strongly resembled those observed on single roughness surfaces of the same diarylethene **1** in previous papers.[7−9] As reported previously, double roughness structures having micro/nanomorphologies show water-droplet-bouncing phenomena that contribute to superhydrophobic and self-cleaning.[4] We thus performed a water-droplet-bouncing experiment from 1.8 mm high on the diarylethene microcrystalline surface with double roughness structures and compared the results with those of diarylethene with single roughness structure and natural lotus leaf (Figure 4). On the lotus leaf, water droplets bounced (Figure 4a; see also

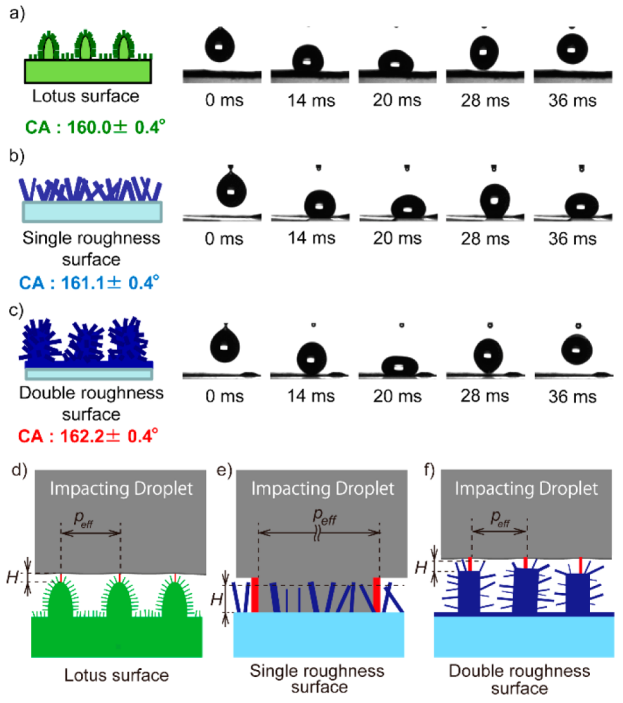

Figure 4. Water-droplet (7.6 μL)-bouncing phenomena on natural lotus leaf (a), diarylethene microcrystalline surfaces with single (b) and double roughness structure (c) (h = 1.8 mm). Schematic representations of Laplace pressure (P_L) on lotus leaf (d), single roughness structure (e) and double roughness structure (f). P_L is determined by height H of surface structures and effective pitches p_{eff} between almost perpendicularly standing needles shown by red.

Supporting Information, Movie 1); by contrast, bouncing was not observed on a diarylethene microcrystalline surface with single roughness structure (Figure 4b; see also Supporting Information, Movie 2).[7−9] Indeed, the phenomenon was reproduced in the diarylethene microcrystalline surface only with double roughness structure (Figure 4c; see also Supporting Information, Movie 3).

This result indicates that these two surfaces even with the same static CA and SA may show differences in bouncing.

Let us consider the reasons why nonbouncing and bouncing are differentiated on the surfaces having the same static CA and SA values. To understand the bouncing on the multipillar surface, the magnitude of Laplace pressure P_L and dynamic pressure P_d provide a clue, where P_L represents the magnitude of suppression factor, and P_d does that of a driving force. If $P_L > P_d$, bouncing occurs. The former is reflecting characteristic sizes of surface structure such as spacing between surface structures $P_L = 16\gamma_L H/(\sqrt{2}p - D)^2$ [γ_L, surface tension; H and D, height and diameter of surface structures; p, pitch between surface structures (see Supporting Information)], whereas the latter is determined by an impacting droplet ($P_d = (1/2)\rho V^2$; ρ, density; V, velocity).[15]

There are three critical points to be taken into account, when we deal with experimental results (Figure 4d−f). (i) The theory cannot be applied directly to the current system because of the randomness of the current surface structure in tilting angle and direction; however, it is possible to estimate the magnitude of P_L from the effective pitch p_{eff} between almost perpendicularly standing crystals on the single roughness and that between the larger-sized structures on double roughness surface and lotus leaf. (ii) p_{eff} could be roughly estimated from the SEM images

DOI: 10.1021/jacs.6b05562
J. Am. Chem. Soc. 2016, 138, 10299−10303

Table 1. Bouncing/Nonbouncing Behavior of Water Droplets from High Positions, with Corresponding P_d Values

h (m)	P_d (Pa)	lotus leaf 2.5×10^3 Pa[a]	single roughness <17.6 Pa[a]	double roughness 1.4×10^3 Pa[a]
0.0018	17.6	yes[b] (Movie S1)	no[c] (Movie S2)	yes (Movie S3)
0.05	490	yes (Movie S4)	no (Movie S5)	yes (Movie S6)
0.10	980	yes (Movie S7)	no (Movie S8)	yes (Movie S9)
0.15	1470	yes (Movie S10)	no (Movie S11)	no (Movie S12)

[a]P_L due to p_{eff} (see Table S1 in Supporting Information). [b]Bouncing occurs. [c]Nonbouncing is observed.

of single and double roughness surfaces and lotus leaf. (iii) The estimated magnitude of P_L can be used as a criterion to determine whether there is nonbouncing or bouncing from the surface structures in comparison with P_d (17.6 Pa). On the single roughness surface, almost all the crystals were tilting; therefore, we could not find suitable needle-shaped crystals. As a result, we concluded that p_{eff} values are over 500 μm (Figure 4e) on a single roughness surface and $P_L < 17.6$ Pa by the above equation using p_{eff} instead of p (Table S1). In contrast, on the double roughness surface and lotus leaf (Figure 4d,f), p_{eff} is estimated to be 35 and 20 μm due to the pitch of the larger-sized structures, respectively (Table S1). Laplace pressure (P_L) due to p_{eff} is estimated to be $1.4-2.5 \times 10^3$ Pa using the above relation. We obtained $P_L > 17.6$ Pa, which explains the bouncing on double roughness surface and lotus leaf consistently. To verify the arguments together with the magnitude of P_L, we carried out further experiments: water droplets (7.0 μL) go down from higher positions h (50, 100, 150 mm; see movies). The magnitudes of P_L and P_d are summarized in Table 1. As a result, the magnitude of P_L is explained by P_d, and the bouncing occurs when P_L is larger than P_d.

We succeeded in generating the double roughness structure. It is a significant advance in mimicking the structural complexity of natural lotus leaves. Actually, the above discussion explains bouncing raindrops on lotus leaf structure (see Supporting Information).[16] By further adjustment to size, height, and spacing, a full reproduction has come into scope. Details are discussed in Supporting Information.

CONCLUSIONS

In summary, we prepared the double roughness structure by using diarylethene **1o** and showed the importance of the double roughness structure on its superwater-repellency by mimicking the structure of a natural lotus leaf. The results support the importance of the double roughness structure to form the water-droplet-bouncing phenomenon which is the origin of self-cleaning on a lotus leaf. The double roughness structure was reversibly photocontrolled by alternate irradiation with UV and visible lights (Figure S9). The diarylethene microcrystalline system can provide versatile surface functions and will be a useful tool for understanding natural surface properties by controlling the sizes of rod- and needle-shaped crystals with changing UV irradiation periods. By using the metal deposition technique, we can immobilize the structures of the surface. Then they will be applicable self-cleaning smart materials for industrial use.

ASSOCIATED CONTENT

Supporting Information

The Supporting Information is available free of charge on the ACS Publications website at DOI: 10.1021/jacs.6b05562.

Experimental details, extended SEM images of the surfaces, average sizes and standard deviations for rod-shaped crystals, size distribution comparison comparison, XRD spectral changes, and theoretical explanation of the bouncing phenomena (PDF)

Video of lotus structure with 1.8 mm bouncing height experiment (AVI)

Video of single roughness structure with 1.8 mm bouncing height experiment (AVI)

Video of double roughness structure with 1.8 mm bouncing height experiment (AVI)

Video of lotus structure with 50 mm bouncing height experiment (AVI)

Video of single roughness structure with 50 mm bouncing height experiment (AVI)

Video of double roughness structure with 50 mm bouncing height experiment (AVI)

Video of lotus structure with 100 mm bouncing height experiment (AVI)

Video of single roughness structure with 100 mm bouncing height experiment (AVI)

Video of double roughness structure with 100 mm bouncing height experiment (AVI)

Video of lotus structure with 150 mm bouncing height experiment (AVI)

Video of single roughness structure with 150 mm bouncing height experiment (AVI)

Video of double roughness structure with 150 mm bouncing height experiment (AVI)

AUTHOR INFORMATION

Corresponding Authors

*mayama@asahikawa-med.ac.jp

*uchida@rins.ryukoku.ac.jp

Notes

The authors declare no competing financial interest.

ACKNOWLEDGMENTS

This work was supported by JSPS KAKENHI Grant JP26107012 in Scientific Research on Innovative Areas "Photosynergetics", JSPS KAKENHI Grant JP26400424 in Scientific Research (C), and the Ministry of Education, Culture, Sports, Science and Technology, Japan (MEXT), as a Supported Program for the Strategic Research Foundation at Private Universities.

REFERENCES

(1) Xia, F.; Jiang, L. *Adv. Mater.* **2008**, *20*, 2842−2858.

(2) (a) Barthlott, W.; Neinhuis, C. *Planta* **1997**, *202*, 1−8. (b) Neinhuis, C.; Barthlott, W. *Ann. Bot.* **1997**, *79*, 667. (c) Gao, X. F.; Jiang, L. *Nature* **2004**, *432*, 36.

(3) (a) Feng, L.; Li, S.; Li, Y.; Li, H.; Zhang, L.; Zhai, J.; Song, Y.; Liu, B.; Jiang, L.; Zhu, D. *Adv. Mater.* **2002**, *14*, 1857−1860. (b) Tian, Y.; Su, B.; Jiang, L. *Adv. Mater.* **2014**, *26*, 6872−6897.

DOI: 10.1021/jacs.6b05562
J. Am. Chem. Soc. 2016, 138, 10299−10303

(4) (a) Lu, Y.; Sathasivam, S.; Song, J.; Crick, C. R.; Carmalt, C. J.; Parkin, I. P. *Science* **2015**, *347*, 1132−1135. (b) Deng, X.; Mammen, L.; Butt, H.-J.; Vollmer, D. *Science* **2012**, *335*, 67−70. (c) Bird, J. C.; Dhiman, R.; Kwon, H.-M.; Varanasi, K. K. *Nature* **2013**, *503*, 385−389. (d) Kwon, Y.; Patankar, N.; Choi, J.; Lee, J. *Langmuir* **2009**, *25*, 6129−6136. (e) Yao, X.; Song, Y.; Jiang, L. *Adv. Mater.* **2011**, *23*, 719−734. (f) Bhushan, B.; Jung, Y. C.; Koch, K. *Philos. Trans. R. Soc., A* **2009**, *367*, 1631−1672. Guo, Z.; Zhou, F.; Hao, J.; Liu, W. *J. Am. Chem. Soc.* **2005**, *127*, 15670−15671.

(5) (a) Sahoo, S. C.; Panda, M. K.; Nath, N. K.; Naumov, P. *J. Am. Chem. Soc.* **2013**, *135*, 12241−12251. (b) Naumov, P.; Sahoo, S. C.; Zakharov, B. A.; Boldyreva, E. V. *Angew. Chem., Int. Ed.* **2013**, *52*, 9990−9995. (c) Naumov, P.; Chizhik, S.; Panda, M. K.; Nath, N. K.; Boldyreva, E. *Chem. Rev.* **2015**, *115*, 12440−12490.

(6) Singleton, T. A.; Burgess, I. B.; Nerger, B. A.; Goulet-Hanssens, A.; Koay, N.; Barrett, C. J.; Aizenberg, J. *Soft Matter* **2014**, *10*, 1325−1328.

(7) Uchida, K.; Izumi, N.; Sukata, S.; Kojima, Y.; Nakamura, S.; Irie, M. *Angew. Chem., Int. Ed.* **2006**, *45*, 6470−6473; *Angew. Chem.* **2006**, *118*, 6620−6623.

(8) Uchida, K.; Nishikawa, N.; Izumi, N.; Yamazoe, S.; Mayama, H.; Kojima, Y.; Yokojima, S.; Nakamura, S.; Tsujii, K.; Irie, M. *Angew. Chem., Int. Ed.* **2010**, *49*, 5942−5944; *Angew. Chem.* **2010**, *122*, 6078−6080.

(9) Nishikawa, N.; Uyama, A.; Kamitanaka, T.; Mayama, H.; Kojima, Y.; Yokojima, S.; Nakamura, S.; Tsujii, K.; Uchida, K. *Chem. - Asian J.* **2011**, *6*, 2400−2406.

(10) (a) Irie, M. *Chem. Rev.* **2000**, *100*, 1685−1716. (b) Irie, M.; Fukaminato, T.; Matsuda, K.; Kobatake, S. *Chem. Rev.* **2014**, *114*, 12174−12277.

(11) (a) Gao, L.; McCarthy, T. J. *Langmuir* **2006**, *22*, 2966−2967. (b) Zhang, J.; Sheng, X.; Jiang, L. *Langmuir* **2009**, *25*, 1371−1376. (c) Feng, L.; Li, S.; Li, Y.; Li, H.; Zhang, L.; Zhai, J.; Song, Y.; Liu, B.; Jiang, L.; Zhu, D. *Adv. Mater.* **2002**, *14*, 1857−1860. (d) Tian, Y.; Su, B.; Jiang, L. *Adv. Mater.* **2014**, *26*, 6872−6897.

(12) (a) Feng, L.; Zhang, Y.; Xi, J.; Zhu, Y.; Wang, N.; Xia, F.; Jiang, L. *Langmuir* **2008**, *24*, 4114−4119. (b) Bormashenko, E.; Stein, T.; Pogreb, R.; Aurbach, D. *J. Phys. Chem. C* **2009**, *113*, 5568−5572.

(13) Yamamoto, M.; Nishikawa, N.; Mayama, H.; Nonomura, Y.; Yokojima, S.; Nakamura, S.; Uchida, K. *Langmuir* **2015**, *31*, 7355−7363.

(14) Nishikawa, N.; Mayama, H.; Nonomura, Y.; Fujinaga, N.; Yokojima, S.; Nakamura, S.; Uchida, K. *Langmuir* **2014**, *30*, 10643−10650.

(15) Jung, Y. C.; Bhushan, B. *Langmuir* **2008**, *24*, 6262−6269.

(16) Mason, B. J. *The Physics of Clouds (Oxford Classic Texts in the Physical Sciences)*, 2nd ed.; Clarendon Press: Oxford, U.K., 2010; p 594.

DOI: 10.1021/jacs.6b05562
J. Am. Chem. Soc. 2016, 138, 10299−10303